# DESIGN FOR ACTIVE FLUTTER SUPPRESION AND MODEL VERIFICATION

Ing. Kratochvíl A.[1], Bc. Svoboda F.[2], Ing. Sommer T. [1], Doc. Ing. Slavík S., CSc. [1],
Faculty of Mechanical Engineering – Czech Technical University in Prague, the Czech Republic [1]
Faculty of Electrical Engineering – Czech Technical University in Prague, the Czech Republic [2]
ales.kratochvil@fs.cvut.cz

***Abstract:*** *The article deals with developing a mathematical model of non-rigid aircraft lifting surface with control surface controlled by pilot and supplementary control surface driven by control law. The purpose of this model is to determine if such as concept of control surface and supplementary control surface can be used for active flutter suppression on an aircraft structure. The supplementary control surface is placed next to the control surface at outboard side. The lifting surface is representing by an airfoil placed at 70% of a wing span.*

*A structural model is developed by means of Lagrange differential equations of second kind. Theodorsen model of thin oscillation airfoil with control surface is used for unsteady aerodynamic. Duhamel's integral of Wagner function is carried out for transformation of unsteady aerodynamic to a time domain. The mathematical model is present in state space representation. There is exemplification of the critical flutter velocity calculation and a dynamical response of the structure. The supplementary control surface for flutter suppression with simplified model is added. Closed-loop feedback control system is formed and a several control laws are presents. The verification of open-loop model is done on behalf of the critical flutter speed comparison with FEM software for flutter analysis MSC.Nastran and flutter analysis program developed at CTU in Prague. The article also presents work on an experimental verification of the open-loop model in aerodynamic tunnel.*

**Keywords**: FLUTTER, ACTIVE SUPPRESSION, STATE SPACE REPRESENTATION, NASTRAN,

## 1. Introduction

Flutter is self-excited oscillation of aircraft structure which leads to complete destruction of an aircraft. It is defined by so called flutter velocity. Above this velocity a damping is positive so amplitude of oscillation increases within the time. Each type of aircraft has to prove that is flutter free up 1,2*Design Velocity of an airplane, before a serial production start. There are several way how to move the flutter to higher velocity. The most common way is by mass balancing or by aerodynamic balancing of control surface. There are also some other ways [1]. A research in area of increasing the flutter velocity of an aircraft structure is aim at active suppression by a control surface to damp an oscillation above the flutter velocity [2] [3]. This paper is aim to verify a new approach of flutter suppression. This approach lies in splitting the control surface in two parts. The inboard part of control surface remains as usual controlled by pilot to maneuver with aircraft. The outboard part of control surface will be driven by control law to suppress undamped oscillation of an airfoil.

## 2. Structural model

The structural model of the airfoil was developed on behalf of Lagrange differential equations of second kind (LDE.II) for three degree of freedom in plunge, pitch and control surface rotation see the model at figure 1. An opposite orientation of coordination system is given by used aerodynamic model.

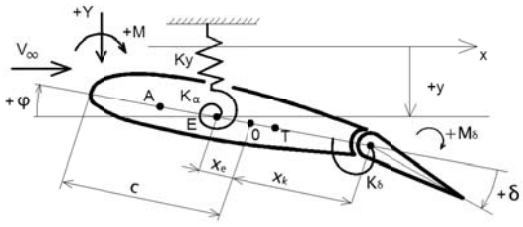


***Fig. 1*** *Model of the airfoil.*

We obtain three differential equation of second order by applying LDE.II. In matrix form written as

$$[M_s]\{\ddot{q}\} + [T_s]\{\dot{q}\} + [K_s]\{q\} = \{F_A\} \quad (1)$$

where $M_s$ - structural mass matrix, $T_s$ - structural damping matrix, $K_s$ - structural stiffness matrix, $F_A$ - vector of unsteady aerodynamic forces and q - deformation vector are defined as follow:

$$q = [y \quad \varphi \quad \delta]^T$$

$$[M_s] = \begin{bmatrix} m & S_{EO} & S_\delta \\ S & J & (x_K - x_E)S_\delta + J_\delta \\ S_\delta & (x_K - x_E)S_\delta + J_\delta & J_\delta \end{bmatrix},$$

$$[T_s] = \begin{bmatrix} b_y & 0 & 0 \\ 0 & b_\varphi & 0 \\ 0 & 0 & b_\delta \end{bmatrix}, [K_s] = \begin{bmatrix} K_y & 0 & 0 \\ 0 & K_\varphi & 0 \\ 0 & 0 & K_\delta \end{bmatrix}, \{F_A\} = \begin{bmatrix} Y \\ M \\ M_\delta \end{bmatrix}$$

where m – is mass, S – static moment, J – moment of inertia, $x_k$ – hinge axis, $x_e$ – elastic axis, b – viscous damping, K – stiffness, y – plunge, φ – pitch, δ – controll surface rotation, Y – lift, M – aerodynamic moment, $M_\delta$ – hinge moment. Because this study is aimed on airfoil investigation without influence of wing span the units of mass matrix and aerodynamic vector are specific.

## 3. Unsteady aerodynamic

The mathematical model of airfoil unsteady aerodynamic forces is based on Theodorsen thin harmonically oscillation airfoil [4]. This model is commonly used for flutter analysis because consider not only aerodynamic forces as a function of free stream velocity but also take in account a change of lift and moment due to airfoil plunge, pitch and control surface rotation.

$$Y = -\rho c^2\left[v\pi\dot{\varphi} + \pi\ddot{y} - \pi c\tilde{x}_e\ddot{\varphi} - vT_4\dot{\delta} - T_1 c\ddot{\varphi}\right] - 2\pi\rho vcC_{(k)}\left[v\varphi + \dot{y} + c\left(\tfrac{1}{2}-\tilde{x}_e\right)\dot{\varphi} + \tfrac{T_{10}}{\pi}v\delta + \tfrac{cT_{11}}{2\pi}\dot{\delta}\right] \quad (2)$$

$$M = -\rho c^2\left[\pi\left(\tfrac{1}{2}-\tilde{x}_e\right)vc\dot{\varphi} + \pi c^2\left(\tfrac{1}{8}+\tilde{x}_e^{\,2}\right)\ddot{\varphi} + (T_4 + T_{10})v^2\delta + \left(T_1 - T_8 - (\tilde{x}_k-\tilde{x}_e)T_4 + \tfrac{T_{11}}{2}\right)vc\dot{\delta} - (T_7 + (\tilde{x}_k-\tilde{x}_e)T_1)c^2\ddot{\delta} - \tilde{x}_e\pi c\ddot{y}\right] + 2\rho vc^2\pi\left(\tilde{x}_e+\tfrac{1}{2}\right)C_{(k)}\left[v\varphi + \dot{y} + c\left(\tfrac{1}{2}-\tilde{x}_e\right)\dot{\varphi} + \tfrac{T_{10}}{\pi}v\delta + \tfrac{cT_{11}}{2\pi}\dot{\delta}\right] \quad (3)$$

$$M_\delta = -\rho c^2\left[\left(-2T_9 - T_1 + T_4\left(\tilde{x}_e - \tfrac{1}{2}\right)\right)vc\dot{\varphi} + 2T_{13}c^2\ddot{\varphi} + \tfrac{v^2}{\pi}(T_5 - T_4T_{10})\delta - \tfrac{vc}{2\pi}T_4T_{11}\dot{\delta} - \tfrac{T_3}{\pi}c^2\ddot{\delta} - T_1c\ddot{y}\right] - \rho vc^2T_{12}C_{(k)}\left[v\varphi + \dot{y} + c\left(\tfrac{1}{2}-\tilde{x}_e\right)\dot{\varphi} + \tfrac{T_{10}}{\pi}v\delta + \tfrac{cT_{11}}{2\pi}\dot{\delta}\right] \quad (4)$$

where $\rho$ – density, c – semichord, v – air stream velocity, $T_{1\div11}$ – Theodorsen constant, $C_{(k)}$ – Theodorsen function. The first group of terms of equations (2) ÷ (4) are called non-circulatory or apparent mass component and they account for inertia of the fluid. The second groups of terms characterized by Theodorsen function C(k) are called circulatory components and they take in account an influence of the shed wake vorticity. Thus the vector of unsteady aerodynamic forces can be written as

(5) $$\{F_a\} = \begin{Bmatrix} Y^{NC} \\ M^{NC} \\ M_\delta{}^{NC} \end{Bmatrix} + \begin{Bmatrix} Y^{C} \\ M^{C} \\ M_\delta{}^{C} \end{Bmatrix} = \{F_a^{NC}\} + \{F_a^{C}\}$$

where $F_a^{NC}$ - non-circulatory part of aerodynamic load *can* be written in form of aerodynamic matrix of mass, damping and stiffness respectively as follow

(6) $$\{F_a^{NC}\} = [M_A]\{\ddot{q}\} + [T_A]\{\dot{q}\} + [K_A]\{q\}$$

The $F_a^C$ - circulatory part of aerodynamic load is

(7) $$\{F_a^C\} = \begin{bmatrix} -2\pi\rho v^2 c \\ 2\pi\rho v^2 c^2\left(\tilde{x}_e + \frac{1}{2}\right) \\ -\rho v^2 c^2 T_{12} \end{bmatrix} C_{(k)} Q_{(t)}$$

Where $Q_{(t)}$- is deformation vector defined as

(8) $$Q_{(t)} = v\varphi + \dot{y} + c\left(\tfrac{1}{2} - \tilde{x}_e\right)\dot{\varphi} + \tfrac{T_{10}}{\pi} v\delta + \tfrac{cT_{11}}{2\pi}\dot{\delta}$$

The term $C_{(k)}$ of equation (7) is in frequency domain and term $Q_{(t)}$ is in time domain. Thus the term $C_{(k)}$ has to be transferred to time domain for purpose of state space model. This can be done on behalf of convolution by means of Duhamel's integral. The Theodorsen and Wagner function are related by mean of Fourier transformation pairs $\psi_{(t)} = \mathrm{C}_{(k)}$ so the Duhamel's integral can be written as

(9) $$\{F_a^C\} = \begin{bmatrix} -2\pi\rho v^2 c \\ 2\pi\rho v^2 c^2\left(\tilde{x}_e + \frac{1}{2}\right) \\ -\rho v^2 c^2 T_{12} \end{bmatrix} \left[ Q_{(t=0)}\psi_{(t)} + \int_0^t \tfrac{\partial Q_{(\tau)}}{\partial \tau}\psi_{(t-\tau)} d\tau \right]$$

An explicit expression for the Wagner function does not exist so for practical evaluation of Duhamel's integral of Wagner function a subsonic approximation by second order exponentials function is used given by [5]

(10) $$\psi_{(t)} \doteq \Phi_{(t)} = 1 - \alpha_1 e^{(-\beta_1 v\, t/c)} - \alpha_2 e^{(-\beta_2 v\, t/c)}$$

$$\alpha_1 = 0.2048 \;\; \alpha_2 = 0.2952 \;\; \beta_1 = 0.0557 \;\; \beta_2 = 0.3330$$

Thanks this approximation the solutions of the Duhamel's integral can be written in state space form as [6]:

(11) $$\begin{bmatrix} \dot{l}_1 \\ \dot{l}_2 \end{bmatrix} = \begin{bmatrix} 0 & 1 \\ -\beta_1\beta_2\left(\frac{v}{c}\right)^2 & -(\beta_1+\beta_2)\left(\frac{v}{c}\right) \end{bmatrix} \begin{bmatrix} l_1 \\ l_2 \end{bmatrix} + \begin{bmatrix} 0 \\ 1 \end{bmatrix} Q_{(t)}$$

(12) $$y_{(t)} = \left[\left(\tfrac{\beta_1\beta_2}{2}\right)\left(\tfrac{v}{c}\right)^2 \quad (\alpha_1\beta_1 + \alpha_2\beta_2)\left(\tfrac{v}{c}\right)\right] \begin{bmatrix} l_1 \\ l_2 \end{bmatrix} + \frac{1}{2} Q_{(t)}$$

or

(13) $$\{\dot{l}\} = [A_2]\{l\} + [B_2]\{u_2\}$$

(14) $$\{y_2\} = [C_2]\{l\} + [D_2]\{u_2\}$$

Where $l_1$, $l_2$ – are an aerodynamic lag states, A – system matrix, B – input matrix, C – output matrix, D – noise matrix, u- input.

## 4. Open-loop model

The open-loop model also called as a system is formed in state space representation by merging the structural model with non-circulatory part of aerodynamic load including a positive feedback formed by circulatory part of aerodynamic loads. The output of the model has to be in form of position, velocity and acceleration for all degree of freedom, for purpose of control law. A schema for model of System is presented at Figure 2.

The structural and aerodynamic model is given as follow:

(15) $$[M_s]\{\ddot{q}\} + [T_s]\{\dot{q}\} + [K_s]\{q\} = \\ = [M_A]\{\ddot{q}\} + [T_A]\{\dot{q}\} + [K_A]\{q\} + \{F_a^C\}$$

by transformation to state space representation we obtain

(16) $$\begin{bmatrix} \dot{x}_1 \\ \dot{x}_2 \end{bmatrix} = \begin{bmatrix} 0 & 1 \\ [M]^{-1}[K] & [M]^{-1}[T] \end{bmatrix} \begin{bmatrix} x_1 \\ x_2 \end{bmatrix} + \begin{bmatrix} 0 \\ [M]^{-1} \end{bmatrix} \{F_a^C\}$$

(17) $$y_1 = \begin{bmatrix} I & 0 \\ 0 & I \\ [M]^{-1}[K] & [M]^{-1}[T] \end{bmatrix} \begin{bmatrix} x_1 \\ x_2 \end{bmatrix} + \begin{bmatrix} 0 \\ 0 \\ [M]^{-1} \end{bmatrix} \{F_a^C\}$$

or

(18) $$\{\dot{x}\} = [A_1]\{x\} + [B_1]\{u_1\}$$

(19) $$\{y_1\} = [C_1]\{x\} + [D_1]\{u_1\}$$

where $M = M_s - M_A$, $T = T_s - T_A$, $K = K_s - K_A$, $x_1 = q$, $x_2 = \dot{q}$,

The circulatory part of aerodynamic load $\{F_a^C\}$ is formed by Duhamel's integral multiple by matrix of aerodynamic constant

(20) $$[K_3] = \begin{bmatrix} -2\pi\rho v^2 c \\ 2\pi\rho v^2 c^2\left(\tilde{x}_e + \frac{1}{2}\right) \\ -\rho v^2 c^2 T_{12} \end{bmatrix}$$

The input to Duhamel's integral represent by Eq. (13) and (14), has to be cut of about second derivation of DOF because they are not needed here. So the following reduction matrix is added in front of Duhamel's integral:

(21) $$[K_Z] = \begin{bmatrix} I & 0 & 0 \\ 0 & I & 0 \end{bmatrix}$$

We can obtain the open loop model of system by merging equations (13), (14), (18), (19), (20), (21) according the schema on figure 2. Then the state space representation of system is

(22) $$\{\dot{x}_{sys}\} = \begin{bmatrix} A_1 + B_1K_3D_2K_ZC_1 & B_1K_3C_2 \\ B_2K_ZC_1 & A_1 \end{bmatrix} \{x_{sys}\} + \begin{bmatrix} B_1 \\ 0 \end{bmatrix} \{u_{sys}\}$$

(23) $$\{y_{sys}\} = [C_1 \quad 0]\{x_{sys}\} + [D_1]\{u_{sys}\}$$

or

(24) $$\{\dot{x}_{sys}\} = [A_{sys}]\{x_{sys}\} + [B_{sys}]\{u_{sys}\}$$

(25) $$\{y_{sys}\} = [C_{sys}]\{x_{sys}\} + [D_{sys}]\{u_{sys}\}$$

with state vector $\{x_{sys}\} = \{x \;\; l\}^T = \{y \;\; \varphi \;\; \delta \;\; \dot{y} \;\; \dot{\varphi} \;\; \dot{\delta} \;\; l_1 \;\; l_2\}^T$

input vector $\{u_{sys}\} = \{0 \quad 0 \quad 0\}^T$

and output vector $\{y_{sys}\} = \{y \;\; \varphi \;\; \delta \;\; \dot{y} \;\; \dot{\varphi} \;\; \dot{\delta} \;\; \ddot{y} \;\; \ddot{\varphi} \;\; \ddot{\delta}\}^T$.

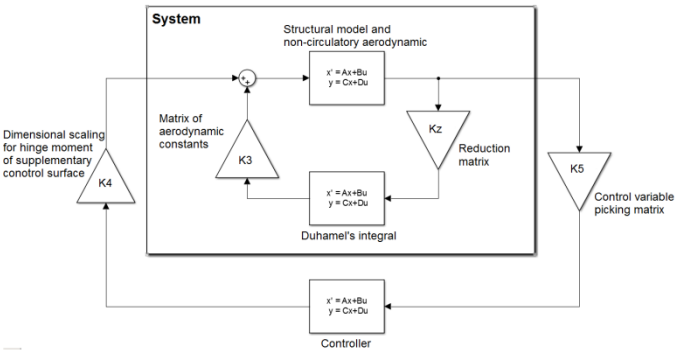


***Fig. 2*** *Schema of the closed-loop model*

## 5. Closed-loop model

There was added the supplementary control surface with controller to the feedback loop of the system. The purpose is an active damping of an airfoil oscillation and shifting the flutter velocity to higher speeds. The supplementary control surface is intangible and non-rigid with aerodynamic load generated on behalf of supplementary control surface rotation Θ only. The transport delays, servo transfer function or sensor noise is not taken in account. This paper is focused on testing if a possibility of the new

concept of flutter suppression is possible at all. The supplementary control surface hinge moment $M_\theta$ is defined as

(26) $$M_\Theta = \frac{1}{2}\rho v_\infty^2 \bar{b}_k c_y^\theta (\bar{x}_k - \bar{x}_e) c^2 \Theta$$

where $\bar{b}_k = \frac{b_k}{2c}$, $c_y^\theta = 2\left(acos\left(1-2\bar{b}_k\right) + 2\bar{b}_k\left(1-2\bar{b}_k\right)\right)$

and will extend equation (5) as follow

(27) $$\{F_a\} = \begin{Bmatrix} Y^{NC} \\ M^{NC} \\ {M_\delta}^{NC} + M_\Theta \end{Bmatrix} + \begin{Bmatrix} Y^C \\ M^C \\ {M_\delta}^C \end{Bmatrix}$$

The angle of rotation Θ will be driven by controller on behalf of the control variable chosen from system output $y_{sys}$. There has to be considered another two gain matrix and state space model for regulator to form the closed loop model. The first matrix is for picking a control variable on behalf of system output

(28) $$[K_5] = [R_1 \;\; R_2 \;\; R_3 \;\; R_4 \;\; R_5 \;\; R_6 \;\; R_7 \;\; R_8 \;\; R_9]$$

Where all constant $R_i$ are zero except the one representing control variable which will be set $\pm 1$ where positive or negative sing is for generating hinge moment in phase or antiphase according to control variable.

The controller transfer function is transform to state space model and added to closed-loop in flowing form

(29) $$\{\dot{z}_R\} = [A_R]\{z_R\} + [B_R]\{u_R\}$$

(30) $$\{y_R\} = [C_R]\{z_R\} + [D_R]\{u_R\}$$

with input as a control variable and output as a supplementary control surface rotation angle $y_R = \Theta$. The second gain matrix

(31) $$[K_4] = \begin{bmatrix} 0 \\ 0 \\ \frac{1}{2}\rho v_\infty^2 \bar{b}_k c_y^\theta (\bar{x}_k - \bar{x}_e) c^2 \end{bmatrix}$$

Generate the supplementary control surface hinge moment on behalf of rotation angle Θ, given by controller. Then the closed-loop model given in figure 2 is defined as follow:

(32) $$\{\dot{x}_{RS}\} = \begin{bmatrix} A_{sys} & B_{sys}K_4C_R \\ B_R K_5 C_{sys} & A_R \end{bmatrix} \begin{Bmatrix} x_{sys} \\ z_R \end{Bmatrix} + [0]\{u_{RS}\}$$

or

(33) $$\{\dot{x}_{RS}\} = [A_{RS}]\{x_{RS}\}$$

(34) $$\{y_{RS}\} = \{y_{sys}\}$$

with state vector $\{x_{RS}\} = \{y \;\; \varphi \;\; \delta \;\; \dot{y} \;\; \dot{\varphi} \;\; \dot{\delta} \;\; l_1 \; l_2 \; z_{R1} \; z_{R2}\}^T$

input vector $\{u_{RS}\} = \{0 \quad 0 \quad 0\}^T$

and output vector $\{y_{RS}\} = \{y \;\; \varphi \;\; \delta \;\; \dot{y} \;\; \dot{\varphi} \;\; \dot{\delta} \;\; \ddot{y} \;\; \ddot{\varphi} \;\; \ddot{\delta}\}^T$.

## 6. Flutter velocity and dynamical response of the model

The velocity of flutter can be obtained by root locus. This is eigen-value analysis of system matrix by:

(35) $$det|A_{RS} - I\lambda| = 0.$$

where $\lambda$ – is eigenvalue. Each eigen-mode is representing by complex conjugate pair of $\lambda = \lambda \pm i\lambda$. The analysis is preform according to the selected variable i.e.: velocity, controller gain and so on. Each λ representing eigen-mode is given as

(36) $$\lambda = \omega(\gamma + i).$$

where $\omega$ – frequency, $\gamma$ – damping, i - complex unit. The lag root obtained by Duhamel's integral has real part only and is defined as

(37) $$\lambda = \gamma_{LAG} \cong -\frac{v_\infty \beta_i}{c}.$$

The flutter velocity is found from complex plot of $\lambda=f(v_\infty)$ where any of eigenvalue cross imaginary axis of complex plot i.e. $Re(\lambda)>0$. The dynamical response of model for given initial condition can be obtained aby solving Eq. (33) and (34).

## 7. Verification of open-loop model

The verification process of system was done for the following input data which are based on data collected during flutter analysis of those airplanes: Sparrow [7], Phoneix [8], Via [9], and Magic [10]. Input data: c=0,475m; $x_e$=-0.238m; $x_k$=0.249m; m=6.814kg/m; $S_{EO}$=0.856kg.m/m; $J_{EO}$=0.630kg.m$^2$/m; $S_\delta$=0.086kg.m/m; $J_\delta$=0.046kg.m$^2$/m; $f_y$=25.6Hz; $f_\varphi$=47.2Hz; $f_\delta$=13.7Hz; $g_y=g_\varphi=g_\delta$=0.03[-]; ρ=1.225kg/m$^3$; where g – structural damping.

The flutter velocity of open-loop model determined by means of root locus Eq. (35) is $V_{FL}$=83.3m/s for plunge. The verification of model derived in this paper was done on behalf of flutter velocity comparison with one obtained by FEM software for flutter analysis MSC.Nastran, flutter analysis program developed at CTU in Prague [11] and author's K-Method [12] for the same input data. The results are listed in table 1.

| Method | MSC.Nastran | K-Method | CTU in Prague | Root locus |
|---|---|---|---|---|
| $V_{FL}$ [m/s] | 84.1m/s | 79.7m/s | 86,5m/s | 83.3 m/s |

***Table 1:*** *Comparison of flutter velocity for different methods.*

## 8. Results of closed-loop analysis

There were tested several type of control laws but only those presented here have some influence on flutter velocity. The main request for control law is to damped an airfoil oscillation to remain in steady flight above open-loop flutter velocity. The controller has to be also design so that does not respond on pilot control inputs for maneuvering of airplane or deformation of aircraft structure caused by turn maneuver. Practically this means not to respond in low frequencies, approximately up to 2Hz. The following table 2 presents the results of analyzed control law and obtained flutter velocities. The table also shows an angular rotation of supplementary control surface as a verification criterion of design correctness.

The results given by Gain controller doesn't satisfy the request not to act in low frequencies. It was used for initial preview into the behavior of the model and for check if the idea of flutter suppression by supplementary control surface is possible. It also show that has to be investigate a positive feedback of controller, given by non-zero constant $R_i$=+1, because the negative feedback caused decreasing the critical flutter velocity in some cases.

The highest closed-loop flutter velocity is for test case ID 11 and 20 with control variable of $\dot{\varphi}$. For this cases the flutter will not occur at all, the critical speed represents a torsional divergence velocity because $Re(\lambda)>0$ for the lag root. But due the unacceptable high rotation of supplementary control surface at low velocity this options can't be used.

The best trade-off between flutter velocity and rotation Θ is test case ID 31 for Band pass controller with $\ddot{y}$ control variable where flutter velocity is 187m/s and Θ=±20° for high velocity and ±40° for low velocity. The root locus and dynamical response of test case ID 31 is on figure 3.

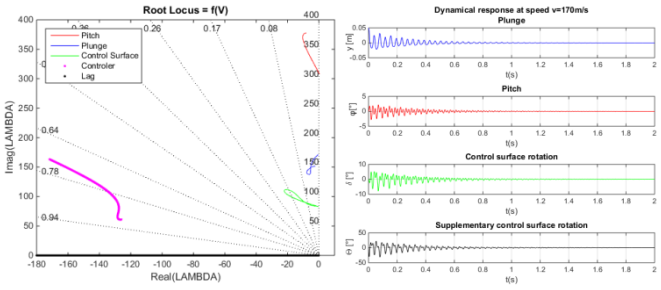

***Fig. 3*** *Root locus and dynamical response for closed-loop test case ID 31*

## 9. Experiment

There was carried out some works on experimental verification of this concept of flutter suppression. A very first model for study of flutter mechanism was built from thin plastic plate. A car was used for execution of an experiment and the flutter occurs at velocity about 16.6m/s.

There was build another experimental model for testing in aerodynamic wind tunnel at CTU in Prague. It was made from balsa and glass fiber composite with reinforcement beam flange from carbon composite. The model had two control surface and one supplementary control surface in the middle driven by controller. Figure 4 show ground vibration test of this model for determining the model input data for mathematical model. This model was destroyed during the experimental determination of open-loop flutter velocity. The problem was to high velocity increment. Construction of another experimental model is in progress.

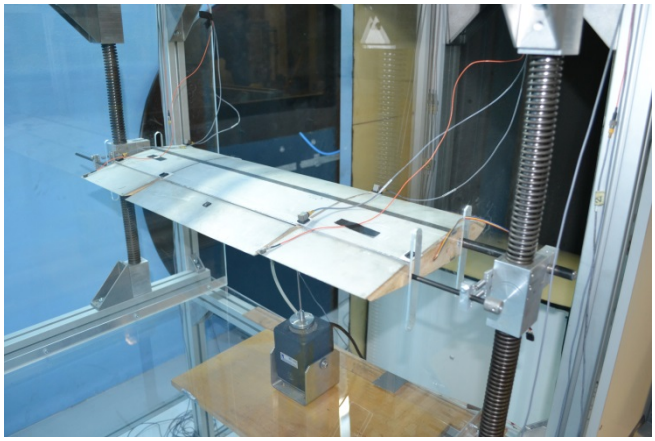

***Fig. 4*** *Ground vibration test of experimental model*

## 10. Conclusion

On behalf of mathematical model derived here the idea of flutter suppression by supplementary control surface can be realized. The analytical calculation shows that the flutter was not suppress but moved to higher velocity only. For the best test cases the velocity was shifted about 225%. Future work on mathematical model will be aimed on inclusion of wing span, unsteady hinge moment of supplementary control surface. There have to be also considered an actuator dynamic and its time delay, sensor location and their noise.

## References

[1] Ramsey, J.G., NASA Aeroelasticity Handbook, Vol.2: Design Guides, Part 2, NASA/TP-2006-212490/VOL2/PART2.
[2] Sutherland, A.N., "A Small Scale Pitch-Plunge Flutter Model for Active Flutter Control Research", 26th International Congress of the Aeronautical Science, 2008.
[3] Karpel, M., "Design for Active Flutter Suppression and Gust Alleviation Using State-Space Aeroelastic Modeling", Journal of Aircraft, Vol. 19, No.3, 1982 p.221-227.
[4] Theodorsen, T., "General Theory of Aerodynamic Instability and the Mechanism of Flutter" NACA Report no. 496, 1935.
[5] Leishman, J. G., Ünsteady Lift of Flapped Airfoil by Indicial Concepts" Journal of Aircraft, Vol.31, No.2, 1994, p. 288-297.
[6] Edwards, J. W., Ashley, H., and Breakwell, J.V., "Unsteady Aerodynamic Modeling for Arbitrary Motions", AIAA Journal, Vol. 17, No. 4, 1979, p.365-374.
[7] Kratochvíl, A., Sommer, T., Slavík, S., „Flutter analysis of wing of the Sparrow-ML" Czech Technical University in Prague, 2013, Report no. VZP/ULT/57/2013
[8] Kratochvíl, A., Sommer, T., Slavík, S., „Flutter analysis of wing of the airplane PHONEIX with 15m wing-span" Czech Technical University in Prague, 2015, Report no. TZP/ULT/9/2015
[9] Kratochvíl, A., Sommer, T., Slavík, S., „Flutter Analysis of the VIA NG6 Airplane" Czech Technical University in Prague, 2015, Report no. TZP/ULT/46/2014
[10] Kratochvíl, A., Sommer, T., Slavík, S., „Flutter analysis of the SR-01 MAGIC UL" Czech Technical University in Prague, 2012, Report no. TZP/ULT/21/2012
[11 Slavík, S., „Direct p-k scheme of wing and empennage flutter characteristics with control surfaces of small sport aircraft", Software, Czech Technical University in Prague, 2010, Id ASW/CLKV/109/2010
[12] Kratochvíl, A., „2D_FlutterModel - 3DOF", Software, Czech Technical University in Prague, 2012, Id ASW/ULT/28/2012

***Table 2:*** *Results from closed-loop analysis*

| ID | Controller transfer function | Control variable | Non-zero constant $R_i$ | Constants of controller | $V_{FL}$[m/s] | Θ[°] $v=0.9V_{FL}$ | Θ[°] $v=0.2V_{FL}$ |
|---|---|---|---|---|---|---|---|
| 1. | Gain controller $TF_G = G$ | y | $R_1 = -1$ | G=16 | 208 | ±30° | ±40° |
| 2. | | $\varphi$ | $R_2 = -1$ | G=24 | 159 | ±50° | ±40° |
| 3. | | $\delta$ | $R_3 = +1$ | G=4.5 | 156 | ±50° | ±60° |
| 4. | | $\dot{y}$ | $R_4 = +1$ | G=3.5 | 33 | ±1000° | ±1000° |
| 5. | | $\dot{\varphi}$ | $R_5 = +1$ | G=0.2 | 84 | ±50° | ±75° |
| 6. | | $\dot{\delta}$ | $R_6 = -1$ | G=0.018 | 91 | ±40° | ±30° |
| 7. | P-I-D controller $TF_{PID} = G\left(1 + T_D s + \frac{1}{T_I s}\right)$ where $T_D=1/\omega_D$ $T_I=1/\omega_I$ | y | $R_1 = -1$ | G=3.00; $\omega_D$ =5; $\omega_I$ =31 | 192 | ±40° | ±50° |
| 8. | | $\varphi$ | $R_2 = -1$ | G=3.08; $\omega_D$ =7; $\omega_I$ =104 | 87 | ±60° | ±60° |
| 9. | | $\delta$ | $R_3 = -1$ | G=0.20; $\omega_D$ =5; $\omega_I$ =500 | 260 | ±40° | ±60° |
| 10. | | $\dot{y}$ | $R_4 = +1$ | G=0.20; $\omega_D$ =19; $\omega_I$ =500 | 120 | ±50° | ±60° |
| 11. | | $\dot{\varphi}$ | $R_5 = +1$ | G=0.03; $\omega_D$ =20; $\omega_I$ =500 | 525 | ±10° | ±90° |
| 12. | | $\dot{\delta}$ | $R_6 = -1$ | G=0.03; $\omega_D$ =120; $\omega_I$=200 | 261 | ±30° | ±80° |
| 13. | | $\ddot{y}$ | $R_7 = +1$ | G=2,1.10$^{-5}$; $\omega_D$=10; $\omega_I$=300 | 87 | ±20° | ±20° |
| 14. | | $\ddot{\varphi}$ | $R_8 = -1$ | G=7,8.10$^{-6}$; $\omega_D$=3,1; $\omega_I$=300 | 85 | ±80° | ±80° |
| 15. | | $\ddot{\delta}$ | $R_9 = -1$ | G=8,0.10$^{-6}$; $\omega_D$=10; $\omega_I$=200 | 86 | ±60° | ±50° |
| 16. | High pass controller $TF_{H-P} = G\frac{Ts}{Ts+1}$ where $T=1/\omega_c$ | y | $R_1 = -1$ | G=30.0; $\omega_C$ =50 | 132 | ±50° | ±50° |
| 17. | | $\varphi$ | $R_2 = -1$ | G=30.0; $\omega_C$ =50 | 94 | ±60° | ±50° |
| 18. | | $\delta$ | $R_3 = -1$ | G=13; $\omega_C$ =150 | 268 | ±60° | ±100° |
| 19. | | $\dot{y}$ | $R_4 = +1$ | G=0.42; $\omega_C$ =250 | 126 | ±50° | ±90° |
| 20. | | $\dot{\varphi}$ | $R_5 = +1$ | G=0.42; $\omega_C$ =250 | 531 | ±35° | ±130° |
| 21. | | $\dot{\delta}$ | $R_6 = -1$ | G=0.04; $\omega_C$ =80 | 261 | ±30° | ±60° |
| 22. | | $\ddot{y}$ | $R_7 = +1$ | G=0.001; $\omega_C$ =100 | 102 | ±50° | ±50° |
| 23. | | $\ddot{\varphi}$ | $R_8 = -1$ | G=0.0045; $\omega_C$ =50 | 85 | ±60° | ±60° |
| 24. | | $\ddot{\delta}$ | $R_9 = -1$ | G=0.0002; $\omega_C$ =50 | 94 | ±100° | ±90° |
| 25. | Band pass controller $TF_{B-P} = G\frac{\omega^2 s}{\omega^2+2\xi s+\omega^2}$ | y | $R_1 = -1$ | G=0.05; $\omega$ =145; $\xi$ =0.3 | 100 | ±30° | ±25° |
| 26. | | $\varphi$ | $R_2 = -1$ | G=0.13; $\omega$ =140; $\xi$ =0.4 | 95 | ±40° | ±20° |
| 27. | | $\delta$ | $R_3 = +1$ | G=0.01; $\omega$ =120; $\xi$ =0.25 | 103 | ±50° | ±30° |
| 28. | | $\dot{y}$ | $R_4 = -1$ | G=1,3.10$^{-4}$; $\omega$ =120; $\xi$ =0.07 | 91 | ±30° | ±15° |
| 29. | | $\dot{\varphi}$ | $R_5 = +1$ | G=1,3.10$^{-4}$; $\omega$ =150; $\xi$ =0.05 | 90 | ±20° | ±15° |
| 30. | | $\dot{\delta}$ | $R_6 = -1$ | G=2,0.10$^{-5}$; $\omega$ =145; $\xi$ =0.05 | 101 | ±50° | ±20° |
| 31. | | $\ddot{y}$ | $R_7 = +1$ | G=0,9.10$^{-5}$; $\omega$ =140; $\xi$ =0.9 | 187 | ±20° | ±40° |
| 32. | | $\ddot{\varphi}$ | $R_8 = -1$ | G=4,0.10$^{-6}$; $\omega$ =150; $\xi$ =0.25 | 85 | ±50° | ±50° |
| 33. | | $\ddot{\delta}$ | $R_9 = -1$ | G=1,0.10$^{-6}$; $\omega$ =120; $\xi$ =0.45 | 106 | ±50° | ±30° |